Analyst

ROYAL SOCIETY OF CHEMISTRY

MINIREVIEW

View Article Online
View Journal | View Issue

Cite this: *Analyst*, 2024, **149**, 3276

Analytical applications of droplet deposition Raman spectroscopy

Eva Kočišová, Alžbeta Kuižová and Marek Procházka *

Received 1st March 2024,
Accepted 4th May 2024

DOI: 10.1039/d4an00336e

rsc.li/analyst

The droplet deposition methods in Raman spectroscopy have received considerable attention in the field of analytical sensing focusing on effective pre-concentration of the studied analyte (coffee-ring effect or small spots). This review covers different analytical applications of drop-coating deposition Raman scattering (DCDRS) and droplet deposition surface-enhanced Raman scattering (SERS) spectroscopy. Two main advantages of droplet deposition Raman techniques are considered: the drying-induced segregation of the components from the mixtures (such as body fluids) and the sensitivity of detection of various analytically important molecules. Some recent advanced applications, including clinical cancer diagnosis, are discussed and summarized. Finally, the potential and further perspectives of the droplet deposition Raman methods for analytical studies are introduced.

1. Introduction

Modern analytical techniques should be highly specific and sufficiently sensitive to detect, identify, and quantify an analyte of interest with minimal requirements for sample pre-treatment and preparation. Raman scattering (RS) spectroscopy is an essential analytical technique for chemical and biological analyses based on the fingerprint chemical/structural information extracted from Raman spectra.[1] The relevant advantages are generally low spectral interference from water as a solvent, minimal need for sample pre-treatment, and non-invasive rapid measurement. However, its serious drawback arises from the inherently weak Raman cross-section of a normal RS (*ca.* 10^{-29} cm^2 per molecule), so relatively high concentrations (>1 mM) and/or large quantities of analyte (>1 μg) are typically required. Surmounting this weakness/difficulty and thus amplifying the Raman cross-section are of utmost importance for the trace detection of abundant analytes in biological samples, contaminants, or pollutants. This can be achieved by surface-enhanced techniques or by an analyte drying-induced pre-concentration effect.

Surface-enhanced Raman scattering (SERS) spectroscopy is an efficient method to obtain enhancement of RS on the order of 10^5–10^{10} for molecules adsorbed on plasmonic (such as gold or silver) nanoparticles (NPs) or nanostructures. In this case, electromagnetic enhancement takes place due to the localised surface plasmon resonance (LSPR) on metal nanostructures. Although SERS has become one of the most sensitive analytical tools with a wide range of applications,[2] it is often not straightforward and generally not applicable for any analyte detection. Another enhancement mechanism, a so-called chemical mechanism (CM), is explained as a charge-transfer between the adsorbed molecule and the surface. This is, for instance, a case involving an analyte dried on a hydrophobic graphene-based substrate known as graphene-enhanced Raman scattering (GERS).[3]

An alternative method for improving the Raman sensitivity is drying-induced pre-concentration of the analyte dropped on a suitable (generally hydrophobic) solid surface. The radially outward flow of a liquid in the evaporating droplet carries the dispersed material of the sample to the edge of the droplet, where it is pre-concentrated in a coffee-ring pattern. An original inspiration for the development of the methods based on the coffee-ring effect was the work by Deegan *et al.* published in the journal *Nature* in 1997.[4] This study brought to mind a commonly known phenomenon when a spilled drop of coffee is evaporated on a solid surface. The process was described based on a capillary flow mechanism and showed that it is due to a geometrical constraint where the free surface, constrained by a pinned contact line, pushes the fluid (with the dispersed material) outwards to compensate for evaporative losses. The edge rings of the pre-concentrated analyte are formed for a wide variety of substrates, dispersed materials (solutes), and carrier liquids (solvents), as long as (1) the solvent meets the surface at a non-zero contact angle, (2) the contact line is pinned to its initial position as is commonly the case, and (3) the solvent evaporates. Moreover, they found that mechanisms typically responsible for solute transport such as surface-tension gradients, solute diffusion, and electrostatic as well as

Charles University, Faculty of Mathematics and Physics, Institute of Physics, Ke Karlovu 5, 121 16 Prague 2, Czech Republic.
E-mail: marek.prochazka@matfyz.cuni.cz

gravity effects are negligible for the ring formation.[4,5] More details on the drying and formation of coffee-ring patterns can be found elsewhere.[6,7]

Combining the coffee-ring effect with detection techniques such as chromatography,[8] colorimetry,[9] mass spectrometry,[10] fluorescence spectroscopy,[11] and Raman spectroscopy brought about various powerful analytical applications.[12] Drop-coating deposition Raman scattering (DCDRS) spectroscopy uses a droplet deposition and evaporation of the target analyte when the Raman spectra are usually measured from the edge of this ring.[13] This way, high-quality Raman spectra can be obtained from samples at small initial volumes (a few μL are sufficient) and several orders of magnitude lower concentrations than in the case of Raman measurement directly from solution or suspension.[13–16]

Although evaporation does not always lead to a coffee-ring pattern, and sometimes small (somewhat spherical) spots are formed, we can benefit from an efficiently pre-concentrated analyte, which is a main prerequisite of the DCDRS approach. Generally, the formed pattern and so the analyte pre-concentration are always the result of the interplay of several factors, such as the type of molecular solution/suspension (analyte), sample concentration and physicochemical properties (contact angles, wettability, and roughness) of the used substrate.[17,18] Various substrates based on hydrophobic top layers such as Teflon-coated stainless steel, polished metals, calcium fluoride (CaF_2), silanised glass, quartz, thiol-modified gold-coated glass or polytetrafluoroethylene tape are successfully used in DCDRS spectroscopy to efficiently pre-concentrate the analyte.[15,16] From the point of view of Raman spectrum acquisition, the substrate itself must have low optical absorbance, the highest possible optical reflectance, and a minimal Raman background signal in the desired spectral region, which is well-ensured in the case of fluorocarbon coatings or polished stainless steel.

The combination of drop-coating deposition with SERS can significantly improve detection sensitivity, benefitting from the synergy of two distinct effects: analyte pre-concentration in a dried pattern (coffee-ring or small spot) and LSPR on the SERS-active surface. Two possible approaches should be taken into consideration: (1) the coffee-ring is formed by dropping and drying the analyte solution on the solid SERS substrate, which ensures SERS enhancement, and (2) the coffee-ring is formed by dropping and drying of the SERS-active NP/analyte mixture on glass/silicon or a similar substrate, so SERS enhancement is ensured by SERS-active NPs. The schematics of DCDRS and both combinations of DCDRS and SERS are depicted in Fig. 1.

This review covers the analytical applications of DCDRS and droplet deposition SERS spectroscopy. Two main advantages of droplet deposition Raman techniques will be considered: the segregation of the components in the mixtures (such as body fluids) and the sensitivity of detection of various analytically important molecules. Some recent advanced applications, including clinical cancer diagnosis, will be summarized. Finally, the potential and further perspectives of the droplet deposition Raman methods for analytical studies will be discussed.

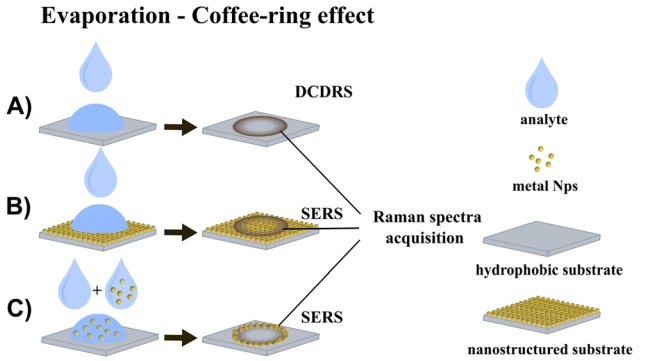

Fig. 1 Schematic figure of (A) DCDRS and (B, C) a combination of droplet deposition with SERS spectroscopy benefitting from the coffee-ring effect where the analyte is dropped on the solid SERS substrate (B) and SERS-active NPs mixed with analyte solution are dropped on the glass/silicon substrate (C).

2. Analytical applications of DCDRS spectroscopy

In the pioneering work of Benz-Amotz *et al.*[13,19] DCDRS was used for the very first time to obtain high-quality Raman spectra of proteins, lysozyme, and insulin, with up to 1000 times higher sensitivity than Raman spectra from solution. Moreover, the authors found that DCDRS spectroscopy benefits from facilitating possible segregation during drying and subsequently enables independent spectral characterisation of the components in the mixture. It was shown to be useful as an efficient approach for separating proteins from other solution components, including fluorescent impurities and buffers.[19] The strength of this method comes from the fact that components in a deposited solution tend to precipitate at different locations on the substrate as a result of a convective streaming during the drying of liquid droplets. This was assumed to be essential for protein accumulation in the edge ring of the dried pattern.[19] In our opinion, the benefits resulting from the segregation capability linked with the coffee-ring effect are still challenging to achieve, and only a few promising studies successfully benefiting from it have been reported.[19–22]

First tests were conducted on single protein and protein/buffer solutions and subsequently on simple protein mixtures. In their first study, Filik and Stone focused on mixtures of three proteins: lysozyme, lactoferrin, and albumin, all of which are commonly found in human body fluids.[20] The aim was to assess the effectiveness of the DCDRS method for determining relative protein concentrations. The study proved that the method is suitable for the compositional analysis of low-concentration protein mixtures and made it possible to assess changes in the relative protein concentrations when subjected to principal component analysis (PCA). This was done with protein levels similar to those in human tear fluid. Moreover,

inhomogeneous deposition of the different proteins during the drying process was also observed. For example, lactoferrin–albumin mixtures were regularly spaced compared to spots from mixtures containing lysozyme, which separated from the other proteins.

The following study was performed on human tears, focusing on determining the components in the tear fluid of healthy volunteers and using Raman point mapping to resolve the spatial distribution of these components in the tear's drying pattern.[23] The DCDRS technique produced good-quality spectra (very high signal-to-noise ratio) collected with short acquisition times and small sample volumes. Raman mapping on the dried deposits revealed the presence of protein, lipid, urea, and bicarbonate, which were inhomogeneously distributed throughout the drying pattern. The positioning of the protein, urea and bicarbonate deposits was related to their relative solubility and concentration. The lipid component was found to never be in solution but visible as debris within the drop.

In the next step, an evaluation of tear fluid analysis by the DCDRS method was developed to determine its potential use as a future medical diagnostic technique.[24] The measured spectra of the tear samples of four volunteers were similar, with only subtle differences between them. Fig. 2 shows a white light image of a section of the tear ring with variation in the concentrations of the proteins separated by filtering urea and CaF_2 across the ring determined by least-squares fitting. The three retentate filtrates from the 100 kDa filter (Ret100), 50 kDa filter (Ret50) and 3 kDa filter (Ret3) were analysed. From the outer edge into the middle of the ring, there is a sharp decrease in the relative contributions of Ret100 and Ret3 compared to that of Ret50. The largest spectral variation from Ret50 shown in Ret3 and Ret100 is the large tryptophan and amide III signal, respectively. In the outer ring mean spectrum, both these features are markedly stronger than those in the inner ring mean spectrum. It is obvious that this approach if combined with determining the tear protein compositions of samples by other techniques (gel electrophoresis or colorimetry) and subsequent advanced data processing by partial least squares (PLS) regression can serve as a possible diagnostic tool.

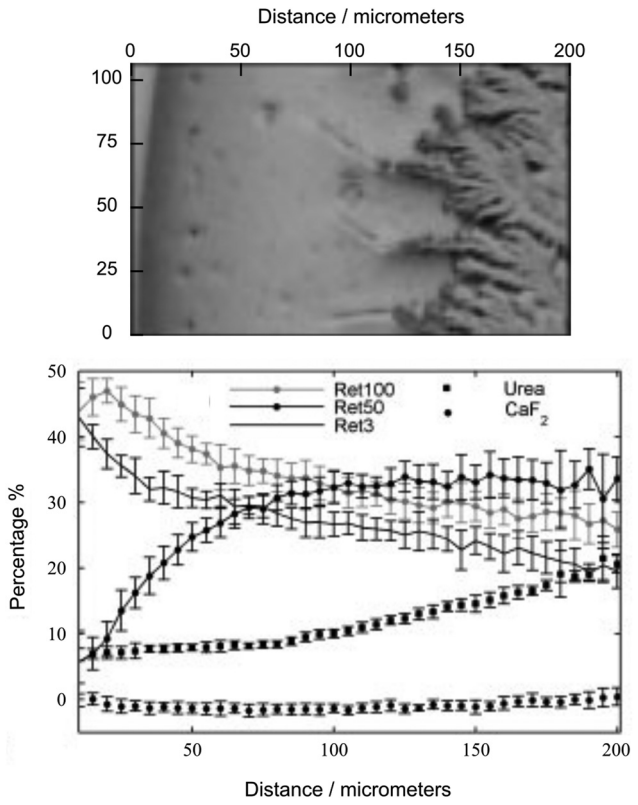

Fig. 2 White light image of the section of the tear ring (top) with variation in the concentrations of the proteins separated by filtering urea and CaF_2 across the ring determined by least-squares fitting (bottom). Adapted from ref. 24 with permission from John Wiley & Sons, Ltd, copyright 2009.

Furthermore, Hu *et al.* employed both DCDRS and SERS spectroscopy to study human tear fluid.[25] They demonstrated that both could be successfully used to analyse the samples without any pretreatment or separation and can provide complementary information about the whole human tear sample. Their results prove that DCDRS is advantageous for the detection of some high-abundance components and SERS for some low-abundance components in the whole tears. They proposed potential further extension also to the analysis of other body fluids.

We employed DCDRS spectroscopy to examine the complex of the cationic copper(II) 5,10,15,20-tetrakis(1-methyl-4-pyridyl) porphyrin (CuTMPyP) and liposomes as a model membrane system, composed of 1,2-dipalmitoyl-*sn*-glycero-3-phosphocholine (DPPC).[26] The measured spectra consisted of the spectral features of DPPC and porphyrins, although the distribution of CuTMPyP in the sample was non-homogeneous. The DCDRS method made it possible to segregate complexed parts from the non-complexed parts of the sample. In addition, the study of the spectra by factor analysis made it possible to distinguish the spectral changes caused by the drying process from the changes caused by the interaction of CuTMPyP with the DPPC liposomes. These spectral changes were attributed to the perturbation of the lipid chain order and porphyrin interaction with the lipid head.

Another experiment in which the CuTMPyP porphyrin/oligonucleotide complex was added to the liposome suspension showed that the drying process caused separation; the liposomes with the bound CuTMPyP porphyrin/oligonucleotide complex were pre-concentrated in the formed edge ring, while the complex itself remained in the central part of the dried pattern. The DCDRS approach also allowed us to reveal that the complexation of oligonucleotides with cationic porphyrin caused its possible binding to the liposome and that this interaction led to certain reorientation of lipid chains.[21]

In addition, DCDRS spectroscopy has been successfully used for the detection of different substances in analytically interesting low concentrations. Djaoued *et al.* studied a domoic acid–tribasic amino acid containing a proline ring,

structurally related to glutamic acid, with a side chain having a conjugated double bond moiety and a hind carboxylic acid.[27] It is naturally present in the marine ecosystem in different locations in the world and is recognised as a neurotoxin. Poisoning can cause short-term memory loss, nausea, difficulty breathing, and coma. The study showed that DCDRS spectroscopy can be applied for the rapid detection of domoic acid down to 25 ng of domoic acid per mL (0.025 ppm). The next study by Dingari *et al.* demonstrated an application of DCDRS spectroscopy to the detection and quantification of the concentration of glycated albumin, which is an important glycaemic marker for long-term diabetes monitoring.[28] Moreover, they were able to accurately discriminate glycated albumin from the unglycated variant, even at low μM concentrations. The reached limit of detection (LOD) for glycated albumin is nearly 4 times lower than the lowest physiological concentrations encountered in practice.

Other important analytes detected by DCDRS spectroscopy were food and agricultural contaminants. In our study, selected contaminants formed small dried spots on a hydrophobic surface making it impossible to obtain Raman spectra from stock solutions under the same experimental conditions.[29] The food contaminant melamine (known as an illegal food additive), fungicide thiram (an animal repellent to protect fruit trees), and herbicides bentazone (applied aerially on food crops to control the spread of weeds occurring amongst the food crops) and picloram (a systemic herbicide used for broadleaf weed control in pasture and rangeland, wheat, barley, oats, and woody plant species) have been studied. DCDRS spectroscopy has been shown to be a powerful method for the detection of these molecules at concentrations relevant to food/groundwater contamination. The lowest detected concentrations were determined as 6.4 μM, 0.31 μM, 20 μM, and 2 μM in deposited concentrations for melamine, thiram, bentazone, and picloram, respectively. Fig. 3A shows the detection of the herbicide bentazone as an example. Although SERS provided better sensitivity for melamine[30] and thiram,[31] no reported SERS study for bentazone and picloram was found in the literature.

We then used the DCDRS approach to explore the drying-induced separation of the main constituents in a melamine-blended milk infant formula.[22] The spatial segregation of lipids and carbohydrates from pure infant formula into a dried pattern was confirmed by Raman spectral mapping. Lipids tended to accumulate in the coffee-ring, and carbohydrates formed a thin layer in the central part of the ring. The same separation in the dried pattern was also observed for the melamine-blended infant formula, where melamine was detected only from the thin central layer together with carbohydrates due to the melamine glycation by lactose depicted in Fig. 3C. We could benefit not only from the efficient pre-concentration and drying-induced spatial separation but also from the chemical reaction potential of molecules of interest present in a complex solution or suspension.

Regarding bacterial studies, dipicolinic acid is an important component of the bacterial spores of the *Bacillus species* and represents ~10% of their dry weight. The spores are dormant and extremely resistant to different environmental stresses. Dipicolinic acid is a principal component of the spore core responsible for this resistance. Using the DCDRS approach, it is possible to detect dipicolinic acid from a 2 μl drop of 5×10^{-7} M deposited concentration as shown in Fig. 3B, which is equivalent to approximately 90 *Bacillus anthracis* spores.[32]

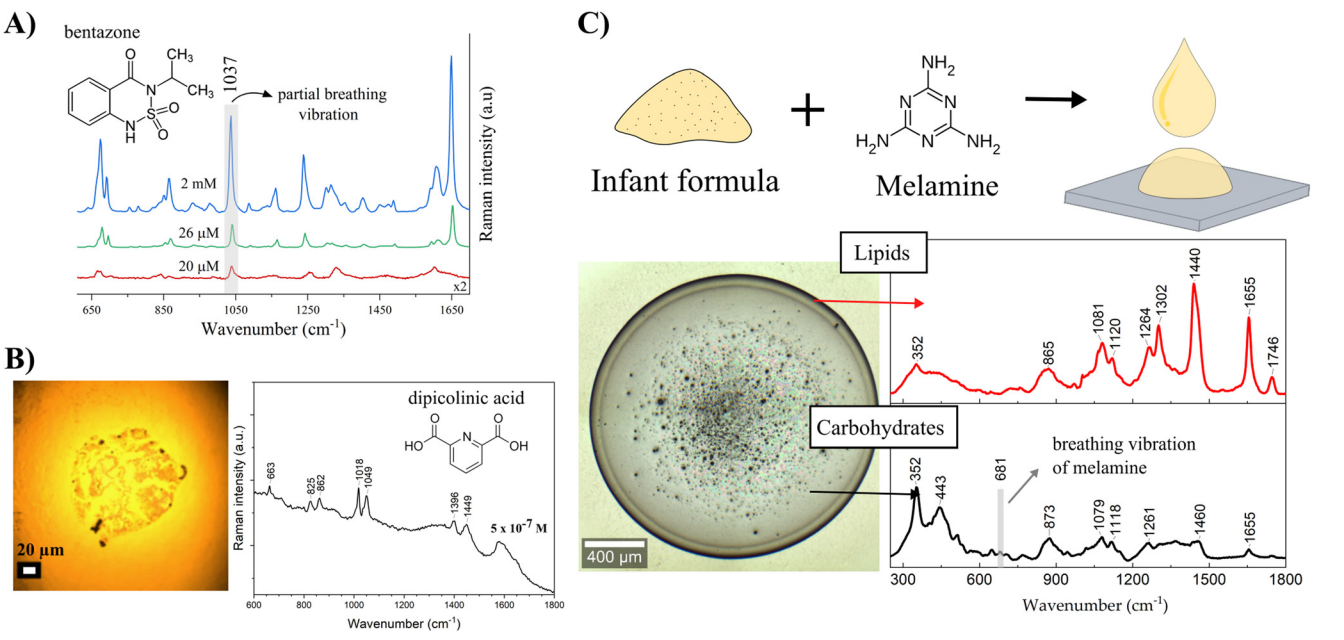

Fig. 3 (A) Detection of the herbicide bentazone by DCDRS spectroscopy. (B) White light image of a dried deposit of dipicolinic acid with the corresponding spectrum. (C) Segregation of lipids and carbohydrates in the dried deposit pattern with the detection of the melamine contaminant only from the layer together with carbohydrates. Inset: chemical structures.

We also used the DCDRS approach to study small molecules with biological importance – acetylsalicylic acid (a substance with antipyretic, anti-inflammatory, and cardio-protective properties), riboflavin (vitamin B2, important in the living cell functioning), and methylene blue (used in different areas of biology and medicine for therapeutic and diagnostic purposes, *e.g.* treatment of methemoglobinemia).[33] The DCDRS detection limits found are 10^{-6}, 10^{-7}, and 10^{-8} M of deposited concentrations for riboflavin, acetylsalicylic acid, and methylene blue, respectively. These detection limits are comparable to or even better than those of the SERS method using the commercial Ag substrate. As for acetylsalicylic acid, no spectra were obtained from concentrations used for the DCDRS approach, probably due to weak adsorption to the silver surface. Moreover, using the DCDRS approach, it was possible to improve the Raman detection sensitivity of porphyrins by a factor of 10^5, and thus, the spectra from ~20 nM deposited concentrations of cationic copper(II) 5,10,15,20-tetrakis(1-methyl-4-pyridyl) porphyrin and anionic copper(II) 5,10,15,20-tetrakis(4-sulfonatophenyl) porphyrin were acquired.[34] Protoporphyrin IX, known as a marker in the clinical diagnosis of cancer, was also detected from a deposited concentration of 10 nM, and although a fluorescence background also appeared, clear Raman bands assigned to the molecule were observed in the spectra.

To profit from DCDRS even more, some studies combined this approach with additional analytical techniques such as chromatography or mass spectrometry. Zhang *et al.* demonstrated the possible compatibility of non-enhanced Raman spectroscopy with chromatographic and mass spectroscopic proteomic sensing on examples of proteomic analytes.[13] They proposed a combined DCDRS/MALDI-TOF approach, providing a mechanism for correlating Raman and mass spectral information. Thus, genetic, environmental, or disease-induced variations in peptides derived from a given protein (with or without posttranslational modifications) could be detected by enzymatic digestion and chromatographic separation followed by DCDRS detection.

Abdolahzadeh *et al.* combined DCDRS spectroscopy with offline monitoring of the reaction's progress.[35] They examined catalysed oxidation of alkenes to epoxides in aqueous solutions at concentrations <10 mM and demonstrated that reproducible spectra can be obtained routinely with relatively little variance, with short acquisition times and sample volumes of 2–10 μL and as little as 1 μg of analyte. The benefit of the DCDRS approach was compared with that of on-line reaction monitoring by ^{1}H NMR and Raman spectroscopy. The authors affirmed the excellent correlation between data obtained from offline and online approaches.

3. Analytical applications of droplet deposition SERS spectroscopy

3.1. Approach 1: analytes dried on a SERS-active substrate

This approach includes all cases where the coffee-ring is formed by dropping and drying the analyte solution on a solid SERS substrate, which ensures SERS enhancement.

Huang *et al.* reported a simple platform, a hydrophobic Ag ink-based plasmonic paper substrate, for simultaneous drop-coating deposition-based pre-concentration and SERS detection of analytes.[36] The hydrophobicity of the plasmonic Ag paper was tuned by Ag-ink concentration to achieve the best pre-concentration of the rhodamine 6G (R6G) analyte in the coffee-ring. Compared with the Raman spectra obtained from conventional DCDRS substrates (such as aluminium), the plasmonic Ag paper offered a much higher Raman signal. From our perspective, dyes like R6G are extensively used in SERS spectroscopy due to their high Raman cross-section value but do not demonstrate the feasibility of the method for real samples with low Raman cross-section value. Although this study did not realise any proof of concept on relevant analytes, it seems that their approach could potentially be a sensitive and label-free detection technique.

Recently, Wi *et al.* introduced a similar platform for the efficient detection of TiO_2 NPs. TiO_2 NPs are widely used as cosmetic additives for blocking UV light and as food additives for artificial colorants.[37] However, there is concern over TiO_2's toxicity. The sensor platform was formed by inkjet-printed porous Ag disks placed on a hydrophobic substrate, such as a hydrogen-terminated Si surface or a fluorosilane-coated glass slide or plastic film (by vapour coating of fluorosilane). A commercial sunscreen lotion (Degussa P25) was dispersed in distilled water and dropped onto the sensor platform. Raman spectra measured from the coffee-ring pattern formed on the Ag disk showed a clear Raman band of TiO_2 at 143 cm^{-1} even at a 0.1 ppb concentration which corresponds to 500 fg of TiO_2. Raman bands belonging to TiO_2 were also identified from the tested chocolate sample, reaching the sensitivity of approximately 200–2000 ppm of TiO_2 (verified by coupled plasma-mass spectroscopy). Since the proposed Raman sensor can be readily prepared by the ink-jet printing of additive-free Ag ion ink, degradation of the Ag nanostructures during storage is avoided.

A distinguished approach is using lithographically fabricated silicon pillar arrays functionalized by Ag NPs for sensitive detection. A dual enhancement of the Raman signals from microdroplets of low-concentration analytes was ensured by combining analyte enrichment through solvent evaporation and plasmonic SERS enhancement. A ≥100-fold concentration of analyte was estimated, with the LOD of 2.9×10^{-12} M for mitoxantrone dihydrochloride.[38] Similar ideas employed superhydrophobic metal needles precoated with SERS-active Ag or Au NPs.[39] This coating step was carried out by pushing the tips through a layer of the NPs confined at a water–oil interface, which resulted in the deposition of a monolayer of NPs on the surface. The NPs were capped with polyvinylpyrrolidone (PVP) to prevent them from jamming together. Then, the small (μL) droplets were dropped to the tip of the needles where they were pinned in place and evaporated, leaving a solid deposit in contact with the SERS enhancing NPs from which the Raman signal is measured. This approach was proved to be extremely sensitive achieving a detection of 2 pg of crystal violet (CV) and 2.5 ng of trinitrotoluene (TNT).[39]

Juneja and Bhattacharya proposed a diagnostic tool to identify low concentrations of noxious pathogens (*Staphylococcus aureus*) from spiked drinking water.[40] They used small pockets of SERS enhancers formed by a 3D Au nanoflower structure on a silicon wafer, providing strong SERS enhancement. To enhance the signal intensities even further, they benefitted from the coffee-ring effect for the pre-concentration of the analytes (water containing *S. aureus*) on such a nanostructure surface. The methodology provided reproducible SERS spectra and the LOD of *S. aureus* in spiked drinking water of 10^3 CFU mL^{-1}. This simple, low-cost, robust, and reproducible method could be useful for increasing the sensitivity of SERS-based detection devices with the capability to be developed into a micro total analysis system.

Liamtsau *et al.* employed the combination of the coffee-ring effect and SERS measurement to study thioarsenicals, such as dimethylmonothioarsinic acid ($DMMTA^V$) and dimethyldithioarsinic acid ($DMDTA^V$), which are important unstable arsenic metabolities.[41,42] The aim was to develop a novel analytical method for the speciation of thiolated arsenicals with minimal sample preparation. They used a Ag nanofilm platform to not only produce the SERS enhancement but to promote the separation of thioarsenic species (Fig. 4). Optimization of the chemical environment (varying pH) resulted in different migration distances of individual species that were together influenced by the radially outward flow of the solute, the thio-arsenical–Ag nanofilm interactions and a thermally induced Marangoni flow. The spatial separation of $DMMTA^V$ to the centre and $DMDTA^V$ to the ring edge of the coffee-ring during the drying process enabled subsequent identification of the species using fingerprint SERS spectra. This work shows how the coffee-ring effect could enable not only the pre-concentration of the studied analyte but also drying-induced spatial separation of different species, which can be further analysed using Raman fingerprint signals. The authors also developed a theoretical framework that adopts a unified approach for both the conventional chromatographic techniques (*e.g.*, GC and HPLC) and coffee-ring-based nanochromatography which employs a stationary phase on the nanometer scale to enable separation at a very short distance (~5 mm). This analysis requires minimal sample pretreatment and allows for nondestructive and simultaneous detection of multiple analytes.[43]

de la O-Cuevas *et al.* combined GERS with DCDRS for sensitive Raman detection of human recombinant interleukin-6 (IL-6) in PBS solution.[44] They successfully used a hybrid platform prepared from a reduced graphene oxide (rGO) thin film deposited on a silicon wafer. The measured signal from the coffee-ring reached a detection limit below 1 pg mL^{-1} with an absolute mass of 1 fg of IL-6. Raman bands acquired from the coffee-ring indicated that IL-6 remains in a solution-like state. In their next study, a combination of DCDRS and GERS was used for specific recognition of the human IL-6 based on the coffee-ring pre-concentration of monoclonal antibodies of IL-6 (mabIL-6) onto an amine functionalized graphene substrate.[45] The formed coffee-ring from the solution of mabIL-6 determined where the selective interaction of the antigen/antibody took place, and IL-6 could be detected and identified by Raman imaging. Fig. 5 (top) shows a scheme of the formation of the substrate: (i) Langmuir–Blodgett (LB) assembly of graphene oxide (GO) substrates (rGO–NH_2 and GO) on a solid support, (ii) drop-coating deposition of mabIL-6 (coffee-ring

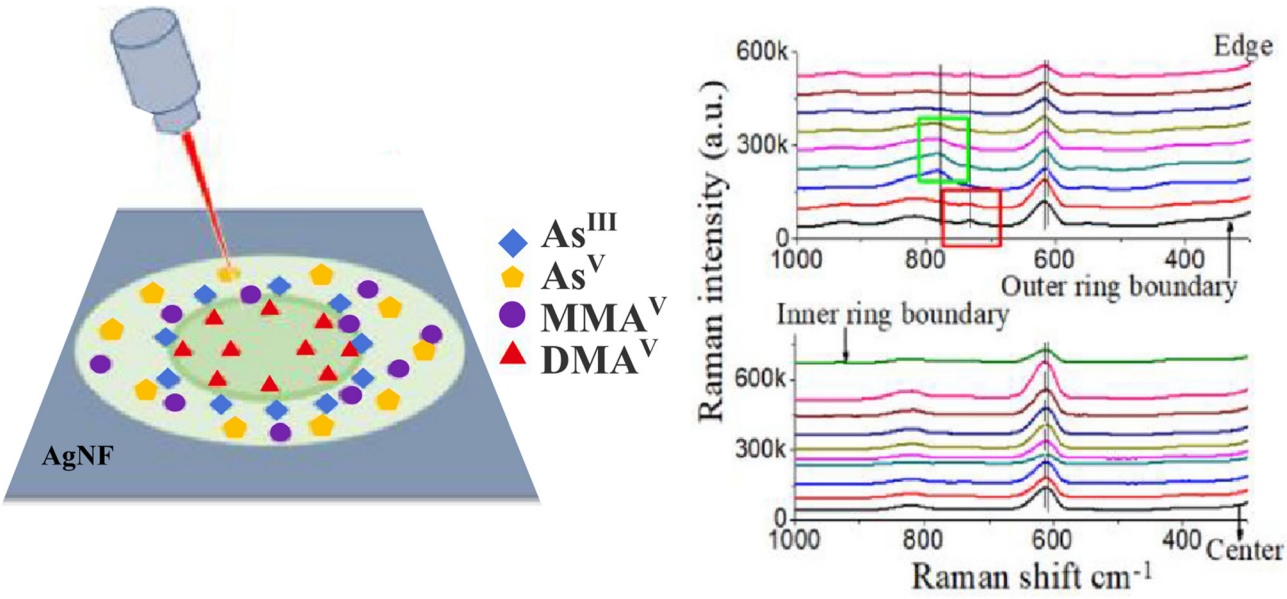

Fig. 4 SERS method for arsenic speciation by using the separation potential of the coffee-ring effect on negatively charged silver nanofilms. (Left) Four arsenic species formed the coffee-ring and (right) the fingerprint SERS signal in solution and on the films. Adapted from ref. 42 with permission from American Chemical Society, copyright 2019.

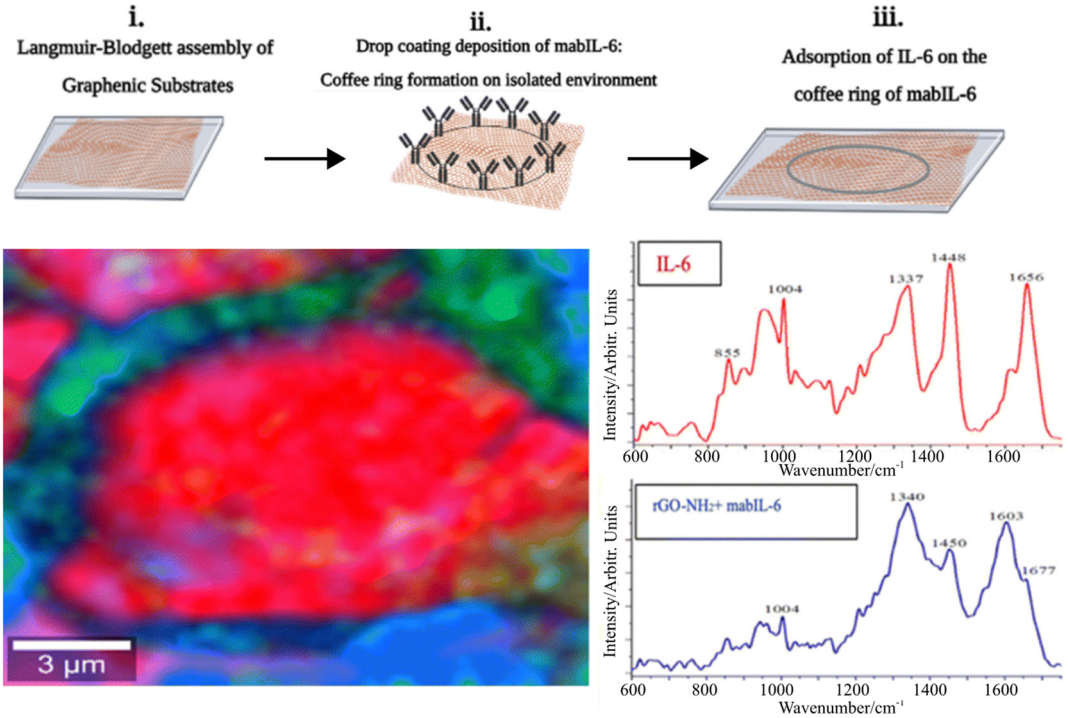

Fig. 5 (Top) Scheme showing (i) the Langmuir–Blodgett (LB) assembly of graphene substrates (rGO–NH_2 and GO) on a solid support, (ii) drop-coating deposition of mabIL-6 (coffee-ring formation) on LB thin films of graphenic substrates and (iii) adsorption of IL-6 on the coffee-ring of mabIL-6. (Bottom) Raman image of the formed coffee-ring and corresponding Raman spectra when the red Raman spectrum is coincident with pure IL-6 and the blue Raman spectrum presents a combination of mabIL-6 and rGO–NH_2 signals. Adapted from ref. 45 with permission from Royal Society of Chemistry, copyright 2023.

formation) on LB thin films of the graphene substrates and (iii) adsorption of IL-6 on the coffee-ring of mabIL-6. Fig. 5 (bottom) shows a Raman image of the formed coffee-ring with Raman spectra when the red Raman spectrum is coincident with pure IL-6 and mabIL-6 and the blue Raman spectrum presents a combination of mabIL-6 and rGO–NH_2 signals. Graphene, prepared by using the chemical vapor deposition technique, served as a substrate where dried drops of the studied amino acids formed coffee-ring patterns.[46] GERS spectra of tryptophan, leucine, phenylalanine, and 3,4-hydroxy-phenylalanine were measured from the ring with the LOD of tens of ng mL^{-1}. Unfortunately, GERS suffers from a low enhancement factor (on the order of 10–20) and in our opinion will not become a routine analytical technique.

3.2. Approach 2: SERS-active NPs/analyte drying on a solid substrate

It is well known that drying of colloidal NPs also forms coffee-ring patterns on certain solid surfaces such as glass/silicon or similar ones.[47] The second approach, the combination of the coffee-ring effect of colloidal metallic NPs and SERS, has received considerable attention thanks to its important applications in the field of analytical sensing.

Our results demonstrated that dried drops of Ag colloid/analyte systems on glass slides formed compact coffee-rings after drying on glass slides.[48–50] We used borohydride-reduced (b.-r.) and hydroxylamine-reduced (h.-r.) Ag NPs with maximum particle size distribution of about 16.8 nm and 38 nm for b.-r. and h.-r. NPs, respectively. The drying process efficiently led to the pre-concentration of the analyte in the ring deposit and promoted the adsorption of the studied analytes to the NPs, as well as creating highly SERS-enhancing sites ('hot-spots'). Thus, by measuring from the ring, SERS spectra that cannot be acquired directly from Ag colloidal solutions (*e.g.* 2×10^{-7} M 1,2-distearoyl-*sn*-glycero-3-phosphocholine – DSPC phospholipid) were obtained.[31] Citrate-reduced (c.-r.) Ag NPs were also tested for the same purpose, allowing the detection of uric acid in solutions down to a 10^{-6} M concentration.[51]

Xu *et al.* developed a SERS sensor for the detection and identification of the environmental pollutants polycyclic aromatic hydrocarbons (PAHs) using bare c.-r. Au NPs (20 nm in size).[52] PAHs are environmental pollutants without any functional group attached to metallic NPs, so direct detection from Ag NPs is impossible. In their tested sensor, a Au NP/PAH mixture dried on a silicon wafer formed the coffee-ring pattern containing closely packed but not aggregated arrays of Au NPs and pre-concentrated PAHs. The SERS spectra of six PAHs, namely, naphthalene, anthracene, pyrene, benzo[*a*]pyrene, benzo[*g*,*h*,*i*]perylene, and indeno[1,2,3-*cd*]pyrene in concentrations down to 5×10^{-6}–2.5×10^{-7} M were obtained by measurement from this coffee-ring pattern. SERS signals collected from 40 spots randomly chosen along each ring demonstrated that the ring provides reproducible and uniform SERS

spectra. To prove the feasibility of detection, the SERS spectra of a sample containing six PAHs in river water matrices were collected using a portable Raman spectrometer, and particular PAHs were identified. This portable SERS sensor provided a robust and versatile approach for simple and direct PAH detection and identification from the environment.

Guo *et al.* introduced an approach combining SERS, chemometrics, and coffee-ring effect to detect patulin (PAT) and alternariol (AOH).[53] PAT and AOH are the main mycotoxin contaminants in fruits and their products, which have great toxic effects on the human body due to their teratogenicity and carcinogenicity. Au nanorods (Au NRs) were mixed with standard PAT and AOH solution and dropped and dried on a silicon wafer to form the coffee-ring pattern (Fig. 6). A stable coffee-ring structure was obtained by optimising the drying temperature and droplet volume. The smoothed and baseline-corrected SERS spectra were analysed using the PLS models to predict the content of PAT and AOH. The best performance was obtained by using the synergy interval and genetic algorithm. The LOD values for PAT and AOH were as low as 1 μg L^{-1}, and the relative standard deviation (RSD) $\leq$ 4.86 for PAT and $\leq$2.28% for AOH. To verify the applicability of their approach, the detection of PAT and AOH in actual apple samples was carried out. Since the number of broken apple cells, soluble polysaccharides, and other substances in apple juice may seriously interfere with signal collection, it was difficult to collect SERS spectra directly from apple juice. Therefore, PAT and AOH were extracted from apple juice samples and detected by SERS and HPLC. The lowest detection concentrations of spiked juice samples were 6.49×10^{-5} mol L^{-1} (PAT) and 3.87×10^{-5} mol L^{-1} (AOH), indicating that SERS combined with the coffee-ring effect had the potential to detect PAT and AOH in real samples quickly and effectively. The SERS technology combined with chemometrics and the coffee-ring effect holds promise for high-throughput label-free detection of PAT and AOH in fruits and their products.

Pan *et al.* prepared a β-cyclodextrin-coated Ag NP to form a coffee-ring for the SERS detection of aromatic compounds such as *o*-phenylenediamine with the LOD of 10^{-10} M.[54] Ag NPs were fabricated, and β-cyclodextrins (β-CD) were physically absorbed on the surface of the Ag NPs as capturing layers of aromatic compounds for enriching the analytes at the interface of the Ag NPs in solution. After the analyte was captured, a mixture of Ag NPs and aromatic compounds was dropped on a silicon wafer to form the coffee-ring from which SERS spectra were acquired.

Ni *et al.* used SiO_2@Ag NPs for SERS-based detection and degradation of target species, including the herbicides paraquat and diquat, and their free radicals.[55] The enhanced Raman signals of these target analytes were achieved through the 'hot-spot' region formed by the self-aggregation of SiO_2@Ag NPs due to the coffee-ring effect. The SERS sensor allowed the detection of the analytes down to 10^{-9} M in the aqueous solution. Recently, Yan *et al.* detected aflatoxin B1 down to 5×10^{-7} M using c.-r. Au NPs.[56]

Wang *et al.* reported the sensitive detection of toxic malachite green (MG) and arsenate based on the Ag NPs and coffee-ring effect.[57] Samples with analytes (from environmental water), Ag NPs, and polyvinyl alcohol (PVA) were vortex mixed, and then the mixture was dripped onto the silicon wafer, where it dried to the coffee-ring pattern. The SERS spectra measured from the ring provided the LOD values of 0.1 ng L^{-1} and 0.03 μg L^{-1} for MG and arsenate, respectively. Since the SERS spectrum is still discriminable even in the MG concentration down to 10^{-12} mol L^{-1} (which corresponds to 25 MG molecules at the laser spot), the authors suggested that this SERS sensor might be applicable for single-molecule detection of MG. Lu *et al.* detected 10^{-15} mol L^{-1} R6G (which also corres-

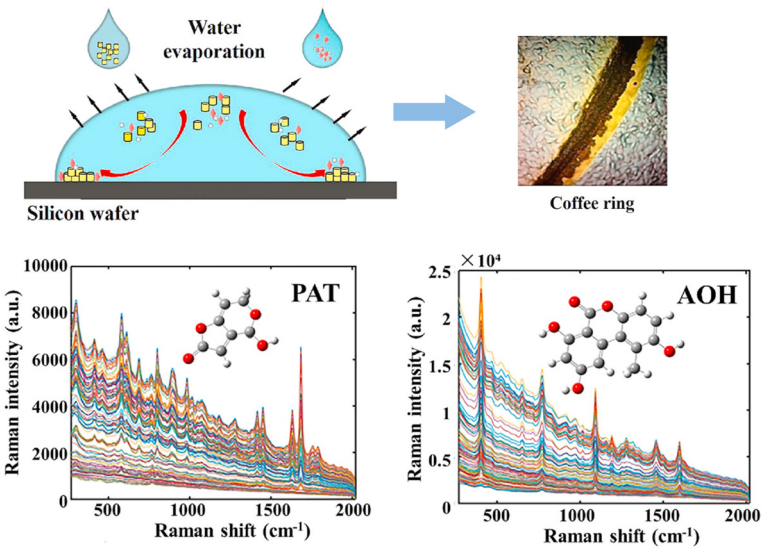

Fig. 6 The high-throughput label-free detection of PAT and AOH using SERS technology based on the coffee-ring effect. Adapted from ref. 53 with permission from Elsevier, copyright 2021.

ponds to the single-molecule level) from Ag NPs dried on a Teflon film.[58] They concluded that Ag NPs dried on the Teflon films exhibit a higher SERS enhancement and better spectral reproducibility compared with that on glass slides.

Wu *et al.* used Ag NPs as the SERS substrate and further employed the coffee-ring effect to detect the illegal adulteration of the chemicals vardenafil and rosiglitazone maleate in healthcare products upto the μg mL^{-1} level.[59] Sodium alginate used as a reduction agent for Ag NP synthesis also protects Ag NPs from aggregation. SERS spectra were measured from the coffee-ring formed by drying the Ag NP/analyte mixture. The method displays a linear response for the determination of vardenafil and rosiglitazone maleate in the 4.88–488 μg mL^{-1} and 4.74–94.7 μg mL^{-1} concentration ranges, and the LOD was as low as 1.63 μg mL^{-1} and 2.20 μg mL^{-1}, respectively. The method was successfully applied to the detection of both analytes in healthcare products, with recoveries higher than 91.52% and RSDs of less than 4.31%.

Regarding medical applications, Hussain *et al.* used Au NPs and Au@Ag NPs with a coffee-ring effect on a gold-coated slide for detecting urea and ammonium sulphate in milk at concentrations down to 5 mg dL^{-1}.[60] This method required a small sample volume and minimal sample treatment. High reproducibility was achieved, confirming that the combination of SERS with coffee-ring effects had the potential to screen other banned and health-hazardous adulterants in milk products simultaneously.

Villa and co-workers reported the pioneering analysis of cancer-relevant biomarkers using the coffee-ring effect of Au NPs.[61,62] The direct deposition of monodisperse Au NPs and *in situ* synthesis of Au NPs on filter paper were used. After that, the analyte adsorption was promoted *via* simple immersion of the SERS substrate in the analyte solution for 30 min. The method displayed in Fig. 7A was successfully applied to the quantitative SERS detection of adenine and guanine in calf thymus DNA after pre-concentration in ring deposit with a calculated value of (G + C)/(A + T) close to the literature value.[61] Later, using this approach, they quantified adenosine (a potential cancer biomarker) in human urine samples.[62] Resolution-alternating least squares (MCR-ALS) were applied to address overlapping bands in the analysis of SERS spectra. The method was shown to be sensitive (the LOD values varying between 3.8 and 4.9 μmol L^{-1}), reproducible (RSD less than ±15%), and selective over other nucleosides (guanosine, cytidine, thymidine, and uridine). This was the first report of a SERS-chemometric method applied to urinary adenosine sensing at physiologically relevant concentrations with minimal sample preparation. Murugesan and Yang used PVP-stabilised Ag NPs mixed with a sample solution.[63] Following the deposition and drying of the mixture solution on a solid substrate, a coffee-ring was formed. When applying the proposed method to determine the phenylalanine level in urine for rapid screening of the phenylketonuria disorder, strong chemical interference from uric acid was observed. To minimise this interference, ZnO powder was applied to the urine sample to adsorb uric acid before SERS detection. Then, SERS signals of phenylalanine were recorded for quantitative purposes. Under the optimised conditions, both the sensitivity and reproducibility of SERS measurement were considerably improved. Quantitative analyses revealed that the developed method is highly feasible for the rapid determination of phenylalanine in real samples. Since adenosine and phenylalanine molecules exhibit high Raman cross-section values, we believe that these approaches are very promising as valuable methods in cancer detection from urine samples.

Hong *et al.* developed a sensor for the rapid diagnosis of colorectal cancer (CRC) through SERS measurements of blood serum.[64] The droplet of a Au NP–serum mixture formed a coffee-ring-like region, providing strong and stable SERS signals. The obtained spectra from cancer patients and healthy volunteers were analysed using unsupervised principal component analysis (PCA) and a supervised machine learning

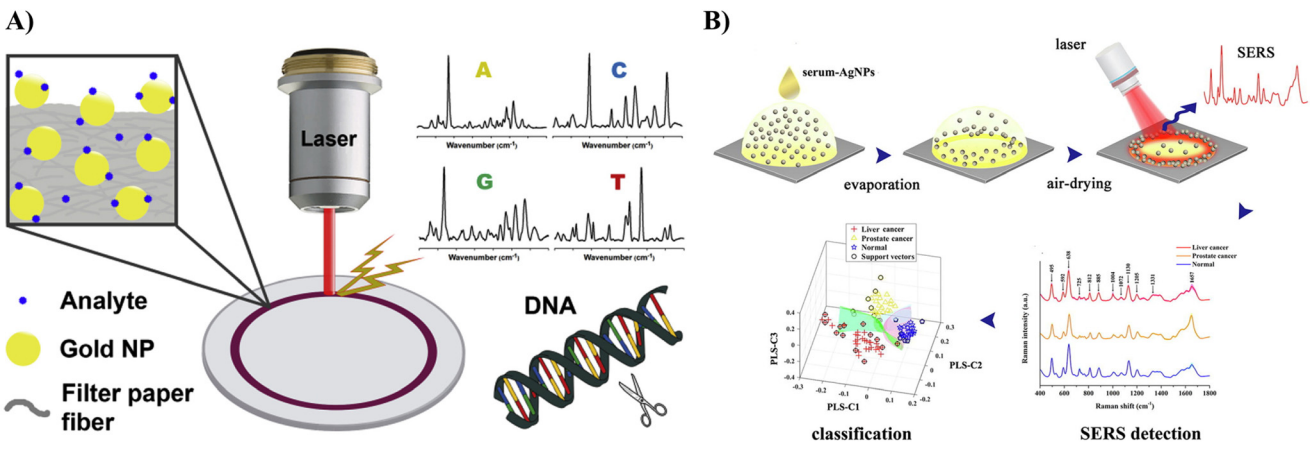

Fig. 7 (A) Quantitative SERS detection of adenine and guanine in calf thymus DNA after pre-concentration due to the coffee-ring effect using the SERS substrate fabricated by *in situ* synthesis of Au NPs on filter paper. Adapted from ref. 61 with permission from Elsevier, copyright 2017. (B) Blood serum analysis strategy using coffee-ring assisted label-free SERS for different types of cancer screening with the corresponding spectra and PLS results for SERS spectral data. Adapted from ref. 65 with permission from Elsevier, copyright 2022.

model, such as support-vector machine (SVM), respectively. The results demonstrate that the SVM model achieves an accuracy and sensitivity of 80% for CRC screening better than that of PCA. Gao *et al.* first used Ag NPs as the SERS substrate combined with a coffee-ring effect for direct label-free blood serum analysis for accurate cancer screening.[65] The unmodified Ag NPs were mixed with the serum from liver cancer patients (n = 40), prostate cancer patients (n = 32) and healthy volunteers (n = 30). The droplets of the Ag NP–serum mixture formed the coffee-ring on the peripheral region after air-drying, providing a stable and reliable SERS signal. Fig. 7B shows typical SERS spectra from the blood serum of liver cancer patients, prostate cancer patients, and healthy volunteers. PLS and SVM algorithms were utilised to establish the diagnosis model for SERS spectral data classification, yielding a high diagnostic accuracy of 98.04% for the healthy group and two types of cancers simultaneously distinguished (Fig. 7B). More importantly, for the unknown testing set, an ideal diagnostic accuracy of 100% could be achieved using the PLS-SVM algorithm for differentiating cancers from the healthy group. The authors stated that the SERS analysis of blood samples combined with the coffee-ring effect and PLS-SVM diagnostic algorithm has the potential for the non-invasive and label-free detection of cancer. Nevertheless, from our point of view, label-free detection of disease markers from blood serum is challenging and may often suffer from low specificity and sensitivity.

3.3. Comparison of both approaches for analytical applications

Two approaches were introduced along with a description of their successful use and application. A comparison of these approaches reveals the advantages and disadvantages of each of them from the point of view of analytical applications.

In approach 1, the dried pattern is formed by dropping and drying the analyte solution on a solid SERS (or GERS) platform, which ensures enhancement of the Raman signal. SERS activity is derived from the SERS-active substrate itself. For the solid, regular, homogeneous SERS-active nanostructure, the signal fluctuation is caused only by the variations of pre-concentration of the analyte in the dry pattern. SERS sensitivity is not as high as in approach 2, but better spectral reproducibility can be achieved. Moreover, in the case of complex analytes and mixtures, approach 1 provides good separation of individual components. Since the SERS effect, in some cases, may be mistaken for a mere coffee-ring effect, a careful evaluation of the measured raw data is necessary.

In approach 2, the dried pattern is formed by dropping and drying the SERS-active NP/analyte mixture on glass/silicon or a similar substrate, so SERS enhancement is ensured by SERS-active NPs. The drying efficiently pre-concentrates the analyte in the ring and promotes adsorption of the studied analyte components to NPs as well as creates 'hot-spots'. The inherent limitation of the drying of NPs is inhomogeneity in sizes of NPs and their aggregates and consequently 'hot-spot' distribution leading to SERS signal alteration and fluctuation. Therefore, this approach offers a high sensitivity but, in some cases, may lack spectral reproducibility. Although some authors reported a stable and reliable SERS signal from dried metal NP/analytes, it seems that achieving satisfactory quantification with this approach remains challenging.

4. Conclusion and further prospects

The droplet deposition Raman spectroscopy considerably improves the Raman sensitivity by drying-induced pre-concentration of the analyte dropped on a suitable (generally hydrophobic) solid surface. The significant advantage is the simplicity and straightforwardness of the technique: only a small sample volume (~μL) and no or minimal sample pre-treatment are needed. The non-enhanced Raman spectrum of the dried analyte deposit provides direct molecular information. Due to segregation capability, the quality of the Raman spectra can be significantly improved as a result of reduced spectral interference from fluorescent impurities and buffer compounds. On the other hand, the separation capability might be limited by the size of molecules and will not work for too small molecules and molecules with high mutual affinity. Moreover, benefitting from the synergy of two distinct effects – analyte pre-concentration in a dried pattern (coffee-ring or small spot) and LSPR in the SERS-active surface – the Raman signal of the analyte can be enhanced even more. In that case, an enhanced SERS spectrum can suffer from signal alteration and fluctuation. Owing to the low enhancement factor (on the order of 10–20), GERS is not suitable for routine analytical applications.

Droplet deposition Raman spectroscopy and its combination with SERS have received considerable attention in the field of analytical sensing. The fundamental applications of droplet deposition Raman techniques include sensitive detection of various analytically important molecules and biomolecules. Moreover, the drying-induced segregation of the components from the mixtures (such as body fluids) represents an important advantage. Chemometric profiting from advanced mathematical tools, *i.e.* PLS regression, should be used to distinguish individual components. There are some exciting advances in body fluid detection combining the coffee-ring effect and SERS technology, where some of such studies focus on the application of the coffee-ring effect-based SERS method to accurately screen cancer in clinical diagnosis. However, the sensitivity and accuracy of simultaneous screening of multiple types of cancer still need to be improved, and further analysed for specific spectral markers linked with individual types of diseases.

The implementation of droplet deposition Raman techniques as routine commercial applications is still challenging. The formation of dried deposits of the target analyte on specific surfaces is generally a complex process and its control is still under investigation. The evaporation of a droplet at room temperature takes around 30 min which brings some limitations, *i.e.* for monitoring fast chemical processes. Moreover, the problematic quantification of the obtained

results is a serious drawback for analytical applications. The outcome should be validated *via* other independent techniques (such as chromatography, colorimetry, or mass spectrometry), not only for quantification but also to prevent potential false positives, especially in the case of disease marker detection. Point-of-care or on-site analysis of droplet deposition Raman spectroscopy could be successfully performed *via* combination with the microarray techniques allowing simple and rapid analysis with high throughput.

Author contributions

Eva Kočišová: writing review/editing and resources; Alžbeta Kuižová: writing review/editing, resources, and visualization; Marek Procházka: writing original draft, resources, supervision, conceptualization, and project administration.

Conflicts of interest

There are no conflicts to declare.

Acknowledgements

Financial support from the Czech Science Foundation (grant GAČR 24-12197S) and Charles University (grant SVV-2023-260716) is acknowledged.

References

1 A. Kudelski, *Talanta*, 2008, **76**, 1–8.
2 M. Procházka, *Surface-Enhanced Raman Spectroscopy. Bioanalytical, Biomolecular and Medical Applications*, Springer, Cham, 1st edn, 2016.
3 X. Ling, L. Xie, Y. Fang, H. Xu, H. Zhang, J. Kong, M. S. Dresselhaus, J. Zhang and Z. Liu, *Nano Lett.*, 2010, **10**, 553–561.
4 R. D. Deegan, O. Bakajin, T. F. Dupont, G. Huber, S. R. Nagel and T. A. Witten, *Nature*, 1997, **389**, 827–829.
5 R. D. Deegan, *Phys. Rev. E: Stat., Nonlinear, Soft Matter Phys.*, 2000, **61**, 475–485.
6 D. Mampallil and H. B. Eral, *Adv. Colloid Interface Sci.*, 2018, **252**, 38–54.
7 M. Parsa, S. Harmand and K. Sefiane, *Adv. Colloid Interface Sci.*, 2018, **254**, 22–47.
8 T.-S. Wong, T.-H. Chen, X. Shen and C.-M. Ho, *Anal. Chem.*, 2011, **83**, 1871–1873.
9 R. Hernandez-Perez, Z. H. Fan and J. L. Garcia-Cordero, *Anal. Chem.*, 2016, **88**, 7312–7317.
10 A. L. M. Marsico, B. Duncan, R. F. Landis, G. Y. Tonga, V. M. Rotello and R. W. Vachet, *Anal. Chem.*, 2017, **89**, 3009–3014.
11 M. K. Fan, C. Z. Huang and Y. F. Li, *Anal. Chim. Acta*, 2002, **453**, 97–104.
12 M. Yang, D. Chen, J. Hu, X. Zheng, Z.-J. Lin and H. Zhu, *Trends Anal. Chem.*, 2022, **157**, 116752.
13 D. Zhang, Y. Xie, M. F. Mrozek, C. Ortiz, V. J. Davisson and D. Ben-Amotz, *Anal. Chem.*, 2003, **75**, 5703–5709.
14 E. Kočišová and M. Procházka, *J. Raman Spectrosc.*, 2011, **42**, 1606–1610.
15 A. Kuižová and E. Kočišová, *J. Raman Spectrosc.*, 2023, **54**, 694–705.
16 E. Kočišová and A. Kuižová, *Appl. Spectrosc. Rev.*, 2024, DOI: **10.1080/05704928.2024.2314534**.
17 E. Kočišová, M. Petr, H. Šípová, O. Kylián and M. Procházka, *Phys. Chem. Chem. Phys.*, 2017, **19**, 388–393.
18 A. Kuižová, A. Kuzminova, O. Kylián and E. Kočišová, *Polymers*, 2021, **13**, 4023.
19 D. Zhang, M. F. Mrozek, Y. Xie and D. Ben-Amotz, *Appl. Spectrosc.*, 2004, **58**, 929–933.
20 J. Filik and N. Stone, *Analyst*, 2007, **132**, 544–550.
21 E. Kočišová, M. Procházka, J. Štepánek and P. Mojzeš, *Spectroscopy*, 2010, **24**, 689749.
22 A. Kuižová and E. Kočišová, *Microchem. J.*, 2024, **199**, 110206.
23 J. Filik and N. Stone, *Anal. Chim. Acta*, 2008, **616**, 177–184.
24 J. Filik and N. Stone, *J. Raman Spectrosc.*, 2009, **40**, 218–224.
25 P. Hu, X.-S. Zheng, C. Zong, M.-H. Li, L.-Y. Zhang, W. Li and B. Ren, *J. Raman Spectrosc.*, 2014, **45**, 565–573.
26 E. Kočišová, M. Procházka and L. Vaculčiaková, *Appl. Spectrosc.*, 2015, **69**, 939–945.
27 Y. Djaoued, S. Balaji and S. Priya, *Spectrochim. Acta, Part A*, 2007, **67**, 1362–1369.
28 N. C. Dingari, G. L. Horowitz, J. W. Kang, R. R. Dasari and I. Barman, *PLoS One*, 2012, **7**, e32406.
29 A. Kuižová, M. Přikryl, M. Procházka and E. Kočišová, *Spectrochim. Acta, Part A*, 2021, **262**, 120109.
30 J. Zheng and L. He, *Compr. Rev. Food Sci. Food Saf.*, 2014, **13**, 317–328.
31 J. Zhu, Q. Chen, F. Y. H. Kutsanedzie, M. Yang, Q. Ouyang and H. Jiang, *Anal. Methods*, 2017, **9**, 6186–6193.
32 E. Kočišová and M. Procházka, *J. Raman Spectrosc.*, 2018, **49**, 2050–2052.
33 E. Kočišová, S. Sayedová and M. Procházka, *J. Raman Spectrosc.*, 2020, **51**, 871–874.
34 E. Kočišová and M. Procházka, *J. Raman Spectrosc.*, 2015, **46**, 280–282.
35 S. Abdolahzadeh, N. M. Boyle, A. Draksharapu, A. C. Dennis, R. Hage, J. W. de Boer and W. R. Browne, *Analyst*, 2013, **138**, 3163–3171.
36 Z. Huang, A. Nagpal, S. Siddhanta and I. Barman, *J. Raman Spectrosc.*, 2018, **49**, 1552–1558.
37 J.-S. Wi, J. D. Kim, W. Lee, H. Choi, M. Kwak, J. Song, T. G. Lee and J. G. Ok, *Int. J. Precis. Eng. Manuf. - Green Technol.*, 2022, **9**, 421–429.
38 R. A. Wallace, J. J. Charlton, T. B. Kirchner, N. V. Lavrik, P. G. Datskos and M. J. Sepaniak, *Anal. Chem.*, 2014, **86**, 11819–11825.

39 C. Li, L. Chai, Q. Chen, Z. Ye, Y. Xu and S. E. J. Bell, *J. Raman Spectrosc.*, 2021, **52**, 386–393.
40 S. Juneja and J. Bhattacharya, *Colloids Surf., B*, 2019, **182**, 110349.
41 V. Liamtsau, C. Fan, G. Liu, A. J. McGoron and Y. Cai, *Anal. Chim. Acta*, 2020, **1106**, 88–95.
42 M. Yang, V. Liamtsau, C. Fan, K. L. Sylvers, A. J. McGoron, G. Liu, F. Fu and Y. Cai, *Anal. Chem.*, 2019, **91**, 8280–8288.
43 V. Liamtsau, G. Liu, A. N. Morozov, A. M. Mebel and Y. Cai, *Talanta*, 2022, **250**, 123688.
44 E. de la O-Cuevas, I. Badillo-Ramírez, S. R. Islas, C. Araujo-Andrade and J. M. Saniger, *RSC Adv.*, 2019, **9**, 12269–12275.
45 E. de la O-Cuevas, S. R. Islas, P. Gallegos-Flores, E. L. Esparza-Ibarra, H. Tototzintle-Huitle and J. M. Saniger, *RSC Adv.*, 2023, **13**, 15114–15120.
46 V. Ranc and Z. Chaloupková, *Analyst*, 2020, **145**, 7701–7708.
47 A. F. Routh, *Rep. Prog. Phys.*, 2013, **76**, 046603.
48 P. Šimáková, M. Procházka and E. Kočišová, *Spectrosc. Int. J.*, 2012, **27**, 393847.
49 P. Šimáková, E. Kocisová and M. Procházka, *J. Raman Spectrosc.*, 2013, **44**, 1479–1482.
50 P. Šimáková, E. Kočišová and M. Procházka, *J. Nanomater.*, 2021, **2021**, 4009352.
51 M. Pucetaite, M. Velicka, J. Pilipavicius, A. Beganskiene, J. Ceponkus and V. Sablinskas, *J. Raman Spectrosc.*, 2016, **47**, 681–686.
52 J. Xu, J. Du, C. Jing, Y. Zhang and J. Cui, *ACS Appl. Mater. Interfaces*, 2014, **6**, 6891–6897.
53 Z. Guo, P. Chen, M. Wang, M. Zuo, H. R. El-Seedi, Q. Chen, J. Shi and X. Zou, *LWT–Food Sci. Technol.*, 2021, **152**, 112333.
54 X. Pan, J. Dong, Y. Li, X. Sun, C. Yuan and W. Qian, *RSC Adv.*, 2016, **6**, 29586–29591.
55 C. Ni, J. Zhao, X. Xia, Z. Wang, X. Zhao, J. Yang, N. Zhang, Y. Yang, H. Zhang and D. Gao, *J. Agric. Food Chem.*, 2022, **70**, 15296–15310.
56 X. Yan, W. Zhu, Y. Wang, Y. Wang, D. Kong and M. Li, *Chemosensors*, 2023, **11**, 22.
57 W. Wang, Y. Yin, Z. Tan and J. Liu, *Nanoscale*, 2014, **6**, 9588–9593.
58 L.-Q. Lu, Y. Zheng, W.-G. Qu, H.-Q. Yu and A.-W. Xu, *J. Mater. Chem.*, 2012, **22**, 20986–20990.
59 J. Wu, L. Zhang, X. Bu, P. Li, B. Zhao and Y. Tian, *Analyst*, 2018, **143**, 5202–5209.
60 A. Hussain, D.-W. Sun and H. Pu, *Food Addit. Contam.: Part A*, 2019, **36**, 851–862.
61 J. E. L. Villa, C. Pasquini and R. J. Poppi, *Anal. Chim. Acta*, 2017, **991**, 95–103.
62 J. E. L. Villa, C. Pasquini and R. J. Poppi, *Talanta*, 2018, **187**, 99–105.
63 B. Murugesan and J. Yang, *ACS Omega*, 2019, **4**, 14928–14936.
64 Y. Hong, Y. Li, L. Huang, W. He, S. Wang, C. Wang, G. Zhou, Y. Chen, X. Zhou, Y. Huang, W. Huang, T. Gong and Z. Zhou, *J. Biophotonics*, 2020, **13**, e201960176.
65 S. Gao, Y. Lin, X. Zhao, J. Gao, S. Xie, W. Gong, Y. Yu and J. Lin, *Spectrochim. Acta, Part A*, 2022, **267**, 120605.